Analyst

PAPER

View Article Online
View Journal | View Issue

Cite this: *Analyst*, 2014, **139**, 3407

FTIR spectroscopy reveals lipid droplets in drug resistant laryngeal carcinoma cells through detection of increased ester vibrational bands intensity†

Sanjica Rak,[a] Tihana De Zan,[a] Jasminka Stefulj,[a] Marin Kosović,[b] Ozren Gamulin*[b] and Maja Osmak*[a]

The major obstacle to successful chemotherapy of cancer patients is drug resistance. Previously we explored the molecular mechanisms of curcumin cross-resistance in carboplatin resistant human laryngeal carcinoma 7T cells. Following curcumin treatment we found a reduction in curcumin accumulation, and reduced induction of reactive oxygen species (ROS) and their downstream effects, compared to parental HEp-2 cells. In order to shed more light on mechanisms involved in drug resistance of 7T cells, in the present study we applied Fourier transform infrared (FTIR) spectroscopy, a technique that provides information about the nature and quantities of all molecules present in the cell. By comparing the spectra from parental HEp-2 cells and their 7T subline, we found an increase in the intensity of ester vibrational bands in 7T cells. This implied an increase in the amount of cholesteryl esters in resistant cells, which we confirmed by an enzymatic assay. Since cholesteryl esters are localized in lipid droplets, we confirmed their higher quantity and serum dependency in 7T cells compared to HEp-2 cells. Moreover, treatment with oleic acid induced more lipid droplets in 7T when compared to HEp-2 cells, as shown by flow cytometry. We can conclude that along with previously determined molecular mechanisms of curcumin resistance in 7T cells, these cells exhibit an increased content of cholesteryl esters and lipid droplets, suggesting an alteration in cellular lipid metabolism as a possible additional mechanism of drug resistance. Furthermore, our results suggest the use of FTIR spectroscopy as a promising technique in drug resistance research.

Received 27th February 2014
Accepted 7th April 2014

DOI: 10.1039/c4an00412d

www.rsc.org/analyst

Introduction

Chemotherapy is one of the principal modes of treatment for cancer patients. Clinically, resistance to chemotherapy is a lack of drug-induced tumor growth inhibition and can arise prior to or as a result of cancer chemotherapy.[1] Cellular, molecular and physiological investigation of the mechanisms underlying drug resistance has identified multiple factors involved in this phenomenon. In general, they include alteration in drug transport and metabolism, mutation and amplification of drug targets, as well as genetic changes which can lead to impaired apoptosis.[1]

Unlike conventional cellular or molecular biology techniques used in cancer research, Fourier transform infrared (FTIR) spectroscopy is developing as a more holistic approach because it gives information about all molecules present in the cell (proteins, lipids, nucleic acids and others). This technique is based on the fact that each molecule has its own distinct pattern of absorption peaks, which can be used as a fingerprint for identification of that molecule.[2] Furthermore, the absorbance peaks are related to the concentration of molecules in a mixture and therefore FTIR spectroscopy can serve as both a qualitative and a semi-quantitative spectroscopic tool. In the past there were some attempts to use FTIR spectroscopy in the study of cancer drug resistance,[3,4] but only in recent years it has become a more popular method in this field of cancer research. Most of the recent studies were aimed at evaluating the potential of this vibrational spectroscopic method to perform cell typing and to differentiate between sensitive and resistant human cancer cell lines.[5–10] This was done with intent to develop FTIR technique as a simple, *in vitro*, reagent-free diagnostic tool for finding drug resistance patterns or predicting the *in vivo* drug response. The FTIR technique also showed

[a]*Division of Molecular Biology, Ruđer Bošković Institute, Bijenička cesta 54, HR-10000 Zagreb, Croatia. E-mail: osmak@irb.hr; Sanjica.Rak@irb.hr; Tihana.De.Zan@irb.hr; Jasminka.Stefulj@irb.hr; Fax: +385-1-4561-177; Tel: +385-1-4560-939*

[b]*Department of Physics and Biophysics, School of Medicine, University of Zagreb, Šalata 3, HR-10000 Zagreb, Croatia. E-mail: ozren@mef.hr; marin.kosovic@mef.hr; Tel: +385-1-4566-797*

† Electronic supplementary information (ESI) available. See DOI: 10.1039/c4an00412d

potential in detecting biochemical changes in tumor cells[11,12] because the results of FTIR analysis were confirmed by other independent methods.[13] In spite of this, only in a few studies was this technique used for the detection of biochemical changes in drug resistant cancer cells in an attempt to get some insights into potential mechanisms of drug resistance.[14,15]

Since resistance of tumor cells to chemotherapy is the major obstacle that limits the effectiveness of cancer treatment, novel strategies that could be efficient against drug resistant tumor cells are being developed such as the use of drugs from traditional medicine. According to the literature, the natural compound curcumin showed the same anticancer effects in several drug resistant cell lines as in their sensitive parental counterparts.[16–19] In our previous work we reported for the first time that drug resistant cells may also be cross-resistant to curcumin.[20] This was shown for the carboplatin resistant 7T cell line that was developed in our laboratory by the treatment of human laryngeal carcinoma (HEp-2) cells with carboplatin.[21] We have previously examined the molecular mechanisms that are involved in the resistance of 7T cells to curcumin and found that following the treatment with curcumin the 7T cells exhibited lower intracellular accumulation of curcumin which coincided with reduced formation of reactive oxygen species (ROS), diminished lipid and DNA damage followed by reduced induction of apoptosis and expression of heat shock protein 70 (Hsp70), as compared to parental HEp-2 cells.[20] In order to get a broader view of all macromolecules involved in curcumin resistance of 7T cells, we decided to use FTIR spectroscopy. We aimed at finding some new potential candidates involved in curcumin resistance that would be further investigated with more specific methods. Here we present that FTIR spectroscopy is able to reveal the presence of specific organelles, lipid droplets, in drug resistant cancer cells through detection of the difference in the ester vibrational band intensity while comparing the spectra of sensitive and resistant cancer cells.

Materials and methods

Cell culture

Human laryngeal carcinoma HEp-2 cells were obtained from the cell culture bank (Gibco, Grand Island, NY, USA). The details regarding the development of their subline resistant to carboplatin (7T cells) have been published previously.[21] These cells were propagated for 26 passages without reversion in sensitivity to carboplatin and have been designated as 7T. HEp-2 and 7T cells were grown at 37 °C with 5% CO_2 as a monolayer culture in Dulbecco's modified Eagle's medium, DMEM (Gibco), supplemented with 10% bovine serum (Gibco). The doubling times for HEp-2 and 7T cells were 22 h and 26 h, respectively.

FTIR spectroscopy

All the measurements were carried out on a PerkinElmer Spectrum GX spectrometer (PerkinElmer, Waltham, Massachusetts, USA) equipped with a liquid N_2-refrigerated MCT (Mercury Cadmium Telluride) detector in an attenuated total reflection (ATR) configuration (for an ATR review, see ref. 22). FTIR-ATR measurements were recorded between 4000 and 450 cm^{-1}. Before scanning the samples the background was recorded by averaging 1000 scans at a resolution of 4 cm^{-1}. Each spectrum of the sample was obtained in about 7 min by averaging 256 scans at a resolution of 4 cm^{-1} and by automatic subtraction of the background.

Due to different doubling times 1.5×10^6 HEp-2 and 1.8×10^6 7T cells were grown in 10 cm dishes for 48 h, when they reached 80% confluency. At that time they were trypsinized, washed three times in isotonic solution (NaCl, 0.9%) to ensure complete removal of trypsin and culture medium (to eliminate their interference in FTIR spectra of cells) and counted. Then the cells were suspended in the NaCl solution at the final concentration of 5×10^5 cells per 20 μl, and placed on ice (2 h maximum) until FTIR spectra were recorded. 20 μl of cell suspension was placed on a ZnSe crystal (dimensions: 50 × 20 mm) by forming the smear that was quickly evaporated in N_2 flux to obtain a homogenous film of cells, as confirmed by microscopic examination. For FTIR measurement we used a horizontal attenuated total reflection (HATR) accessory for a PerkinElmer Spectrum GX spectrometer with the angle of reflection of 45 degrees and the beam reflected 12 times. In two separate experiments three independent dishes were grown for each cell line, and three to four samples were taken from each dish for infrared measurements, thus generating a total of 18–20 spectra per cell line. After 3–4 spectra of each dish were taken, cell viability (of remainder of cell suspension that was kept on ice) was evaluated by trypan blue staining and it was 95% *i.e.* the same as before the cells were placed on ice.

FTIR data analysis

To obtain information about the differences between the recorded spectra, principal component analysis (PCA) was performed using the Matlab add-on PLS Toolbox (Eigenvector Research, Inc., Wenatchee, Washington USA). Since 18–20 spectra were recorded per each cell line, and each wavelength is a variable, the total number of variables that has to be compared with statistical analysis is extremely large. These data are therefore best processed with PCA statistical analysis, an unsupervised statistical method that enables the reduction of variables by building linear combinations of wavenumbers that vary together. The first principal component (PC 1) accounts for most variance present in the dataset and the second (PC 2) is built with the residual variance and is uncorrelated to the first one.[23] Mean center preprocessing was applied on all spectra before PCA.

The second method to explore the differences between the recorded spectra was hierarchical classification of the spectra. It gives information about spectral relationships or spectral similarities which are presented in the form of a dendrogram constructed with Ward's algorithm. Shortly, the Euclidean distance between all the recorded spectra is calculated and the closest spectra are linked to form a group. For hierarchical classification analysis we used the same Matlab add-on and mean center preprocessing as for PCA.

To gain more insight into the chemical differences between parental HEp-2 and resistant 7T cell lines another statistical method, Student's *t*-test, was used. The spectra were processed with the specific "homemade" software Kinetics (the kind gift of Prof. E. Goormaghtigh) which runs under Matlab 7.[24] The recorded spectra were first baseline corrected and then normalized to the maximum intensity of the amide I band. To obtain the difference spectra, the mean spectra of the parental HEp-2 cell line were subtracted from the mean spectra of the resistant 7T line. The positive and negative peaks in the difference spectra are representative of the molecules that are relatively more abundant (positive peaks) or less abundant (negative peaks) in 7T cells.[23] The obtained difference spectra were analyzed using Student's *t*-test which was performed for each point in spectra in order to extract the spectral regions where statistically significant differences ($p < 0.05$) between two cell lines were observed. Wavenumbers where a significant difference occurred were indicated by thicker lines.

Quantification of cholesteryl esters by enzymatic assay

For quantification of cholesteryl esters, HEp-2 (2×10^5 per well) and 7T cells (3×10^5 per well) were grown in 6-well plates and 48 h after seeding they were washed with PBS and lysed in a buffer containing 50 mM Tris–HCl (pH 7.6), 150 mM NaCl, 2 mM EDTA, 1% NP40, 0.5% Triton X-100 and protease inhibitor cocktail (Sigma-Aldrich, Seelze, Germany). Cell lysates were centrifuged at 16 000*g* for 10 min at 4 °C. The cholesterol content in the supernatants was determined using the Amplex Red Cholesterol Assay Kit (Molecular Probes, Invitrogen, Eugene, Oregon, USA) according to the manufacturer's protocol. Fluorescence of resorufin (530 nm excitation/590 nm emission wavelengths) was measured using a microplate fluorometer Fluoroskan Ascent FL (Thermo Electron Corporation, Waltham, Massachusetts, USA). The total and free cholesterol amounts were determined by performing the assay in the presence and absence of cholesterol esterase (50 units per ml), respectively. The cholesterol mass in cholesteryl esters was determined by subtracting the free cholesterol values from the total cholesterol values. These values were normalized to the total protein content, as measured by the Bradford method.

Oil Red O staining of lipid droplets

HEp-2 (4×10^4 per well) and 7T (6×10^4 per well) cells were plated in a 24 well plate and 24 h after seeding the cells were incubated for an additional 24 h with or without serum. Thereafter they were washed two times with PBS and fixed for 30 min with 4% paraformaldehyde. After washing with dH_2O and 60% isopropanol they were dried and stained for 10 min with Oil Red O (Sigma-Aldrich) solution (6 : 4 ratio of 0.3% stock Oil Red O in dH_2O). Thereafter they were counter-stained with haematoxylin for one minute. After extensive washing with tap water, cells were dried, covered with mounting media and examined for lipid inclusions with an Axiovert 35 microscope (Zeiss, Oberkochen, Germany). Images were taken with the camera Pixera Pro150ES (Pixera Corporation, San Jose, California, USA).

Nile Red staining and flow cytometry

HEp-2 (2×10^5 per well) and 7T cells (3×10^5 per well) were grown in 6-well plates and 24 h after seeding they were incubated for an additional 24 h with serum, without serum or with 200 μM oleic acid (Sigma-Aldrich). After the treatment cells were collected by trypsinization and washed with warm PBS without Ca^{2+} and Mg^{2+} ions (to prevent cells from clotting). Thereafter they were stained with 0.1 μg ml^{-1} Nile Red solution, prepared in the washing buffer from 1 mg ml^{-1} stock of Nile Red in DMSO, and incubated for 30 min at room temperature while being protected from light. After washing with cold PBS without Ca^{2+} and Mg^{2+} ions, cells were resuspended in the same buffer and kept on ice until analysis with a FACSCalibur flow cytometer (Becton Dickinson, New Jersey, USA). FL1 green fluorescence from 10 000 cells was monitored because Nile Red is a lipophilic dye whose green fluorescence is specific for binding lipid droplets due to their reduced polarity compared to cell membranes.[25]

Statistics

The results were presented as mean ± standard error of the mean (SEM). The two-sided paired Student's *t*-test was performed to evaluate the significance of the differences between the HEp-2 and 7T cells. *p* values less than 0.05 were accepted as significantly different.

Results

PCA statistical analysis

In FTIR spectra that were recorded from parental HEp-2 and resistant 7T cells (see ESI in Fig. S1†) changes are not easily noticed without the statistical analysis. Therefore, in order to see if there are any spectral differences regarding the whole absorbing region (3100–1000 cm^{-1}), PCA statistical analysis was applied to compare the two cell lines. The results of PCA statistical analysis on all individual spectra of HEp-2 and 7T cells are reported in Fig. 1 as a projection of the spectra in the first two principal components. The percentage between brackets represents the fraction of total variance described by the principal component (PC). More than 91% of spectral variance was explained by the first (PC 1) and second principal component (PC 2). As evident from Fig. 1, the clear separation between HEp-2 and 7T cell lines is obtained in the principal components PC1–PC2 space, suggesting a clear difference between FTIR spectra of parental HEp-2 cells compared to resistant 7T cells regarding the whole absorbing region.

Hierarchical classification of all recorded spectra

To verify the results of PCA statistical analysis we used a hierarchical classification of all recorded spectra. By using this method we were able to get information about the similarities between all recorded spectra regarding the whole absorbing region (3100–1000 cm^{-1}). As shown in Fig. 2 two major classes of spectra emerged after hierarchical classification of data. One class corresponded to the spectra of parental HEp-2 cells and the other to the spectra of the resistant 7T cells. This clear

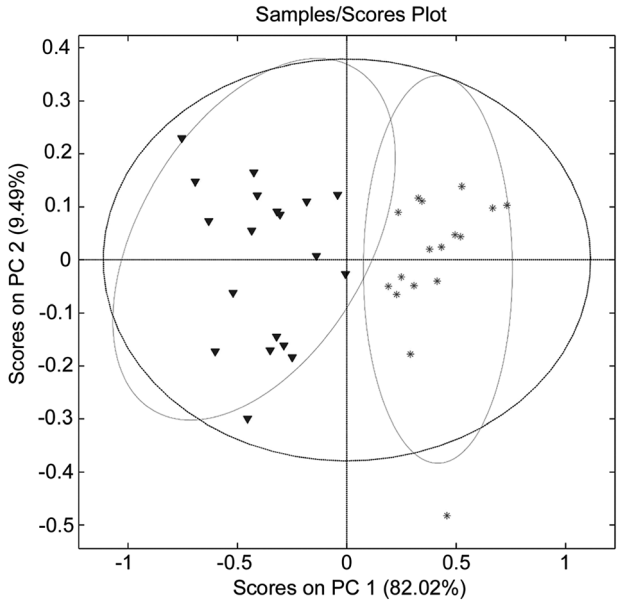

Fig. 1 PCA of all recorded HEp-2 and 7T spectra. Each point of the plot is a projection of a spectrum in the principal component PC1–PC2 space. Lighter dots represent HEp-2 spectra and dark triangles represent 7T spectra. Ellipses depicted in the figure define confidence limits, within which 95% of the data are allocated. The spectral range used for this analysis was: 3100–1000 cm^{-1}.

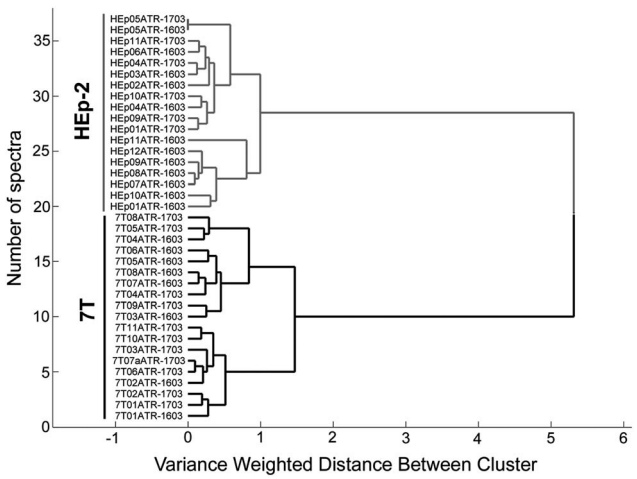

Fig. 2 Hierarchical classification of all recorded HEp-2 and 7T spectra. The spectral range used for this analysis was 3100–1000 cm^{-1}.

separation showed that there is an evident difference between HEp-2 and 7T recorded spectra when taking the whole absorbing region into account.

Student's *t*-test of HEp-2 and 7T difference spectra

Since HEp-2 and 7T recorded spectra are evidently different with regard to the whole absorbing region, we wanted to identify at which wavenumbers these differences are statistically significant. For this purpose difference spectra from HEp-2 and 7T mean spectra were obtained and analyzed with Student's *t*-test at each wavenumber. The result is shown in Fig. 3. Five

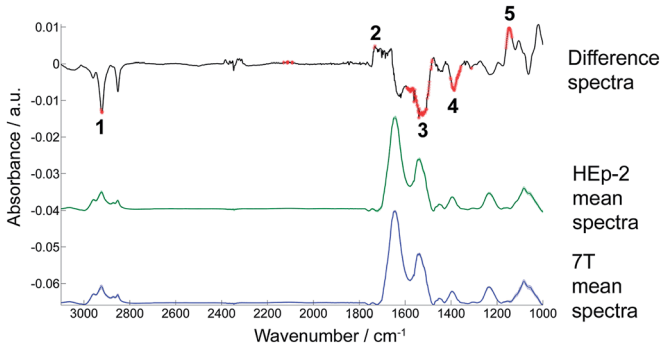

Fig. 3 Difference spectra obtained by subtraction of 7T mean spectra from HEp-2 mean spectra. A Student's *t*-test was computed at every wavenumber with a significance level of $p < 0.05$. Statistically significant difference between the means was marked with a thicker red line and they are numbered according to the band assignments based on the literature. For numeral annotations (1–5) see the description in Table 1.

different regions (peaks) were marked with a thicker red line because a statistically significant difference ($p < 0.05$) between HEp-2 and 7T mean spectra was observed at those points. For verification of these results additional PCA statistical analysis was done (see ESI in Fig. S2†). These statistically different peaks (spanning one or more wavenumbers) were marked with numbers from 1 to 5 and given band assignments based on the literature[2,10,23,26–31] (Table 1). Positive and negative contributions of these peaks in the difference spectra gave us information about the molecules that are relatively more abundant (positive peaks) or less abundant (negative peaks) in resistant 7T cells. Peaks with numbers 1, 3 and 4 are negative while peaks 2 and 5 are positive. According to the band assignments from Table 1, it can be interpreted that there is a lesser abundance of lipids (peaks 1 and 4) and proteins (peaks 3 and 4) in the resistant 7T cell line compared to parental HEp-2 cells. On the other hand, 7T cells have a greater abundance of cholesteryl esters because

Table 1 Band assignments based on the literature[2,10,23,26–31] for wavenumbers where significant changes in FTIR difference spectra of the laryngeal carcinoma parental and resistant cell line were detected

Peak no.	Wavenumber (cm^{-1})	Spectral assignment
1	~2921	CH_2 asymmetric stretching mainly from lipids, with little contribution from proteins, carbohydrates, nucleic acids
2	~1735	C=O ester stretch from cholesteryl esters, triglycerides, phospholipids
3	~1530	Amide II (N–H bending, C–N stretching from proteins)
4	1400–1340	COO^- symmetric stretching from fatty acids and amino acids, CH_3 symmetric banding from lipids, CH_2 wagging from phospholipids, fatty acids, triglycerides and amino acids side chain
5	1170–1130	CO–O–C asymmetric stretching from cholesteryl esters, glycogen and nucleic acids

of the positive orientation of peaks 2 and 5 (Table 1). We reached this conclusion because these two peaks, among other assignments, have one mutual assignment with cholesteryl esters. Other possible assignments, *i.e.* phospholipids and triglycerides, are not so straightforward because of different orientation of other peaks also assigned to this type of molecule (see Table 1, peaks 1 and 4).

In conclusion, the data of Student's *t*-test analysis showed the reduced levels of lipids and proteins (which represent two quite broad groups of molecules) and an increase in the cholesteryl ester content in resistant 7T cells compared to parental HEp-2 cells.

Detection of higher cholesteryl ester levels in resistant 7T cells by enzymatic assay

The most straightforward results of FTIR spectral analysis showed that the resistant 7T cells have an increased amount of cholesteryl esters compared to parental HEp-2 cells. Because of the potential biological significance of these data we verified this result by using a specific fluorometric enzymatic method which can detect very low concentrations of cholesterol. This assay measures total and free cholesterol, and the amount of cholesteryl esters is determined as the difference between the total and free cholesterol levels.

The result of enzymatic assay (Fig. 4) showed that, although the quantity of cholesteryl esters in both cell lines was quite low (around 0.4 μg mg^{-1} of protein for HEp-2 cells and 0.8 μg mg^{-1} of protein for 7T cells) (Fig. 4A) compared to quantities of free cholesterol (around 3.2 μg mg^{-1} of protein for HEp-2 and 7T cells) (Fig. 4B), the amount of cholesteryl esters is indeed increased in resistant 7T cells and is almost two times higher compared to the amount in HEp-2 cells (Fig. 4A). In contrast, the amount of free cholesterol is the same in both cell lines (Fig. 4B). Since the amount of cholesteryl esters in 7T cells was increased, the total cholesterol amount was also slightly increased compared to HEp-2 cells (Fig. 4C). However, since the cholesteryl ester quantity was quite low, this difference was not statistically significant.

Detection of lipid droplets in resistant 7T cells

According to the literature, cholesteryl esters are molecules localized in special cytoplasmic organelles called lipid droplets (LDs). They are composed of a lipid core which contains mainly cholesteryl esters and triglycerides in various ratios and surrounded by a lipid monolayer composed of phospholipids and proteins.[32] Cells can form LDs if lipids are available in the growth medium. When maintained under serum-deprived conditions, LDs practically disappear. However, LDs can be induced if free fatty acids are added to the growth medium at nontoxic concentrations.[33]

In order to examine the presence of LDs in HEp-2 and 7T cells, we used two hydrophobic dyes: Oil Red O and Nile Red,

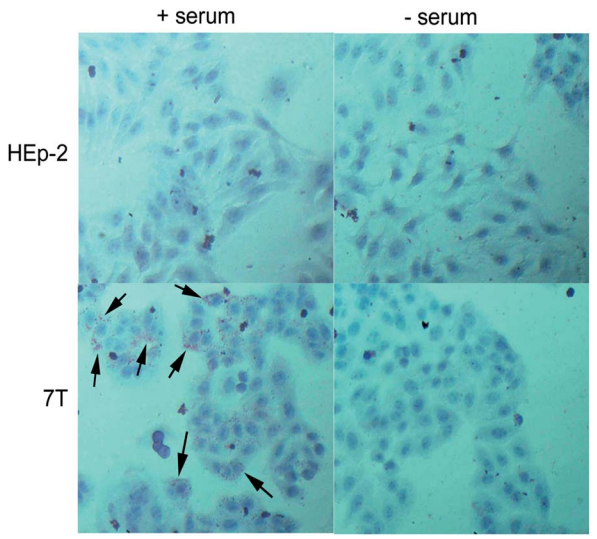

Fig. 5 Oil Red O staining of lipid droplets in HEp-2 and 7T cells. 24 h after the seeding cells were incubated in a growth medium for an additional 24 h with or without serum, fixed and stained with Oil Red O and haematoxylin. Arrows indicate red colored lipid droplets inside 7T cells. The pictures were taken at a magnification of 200×.

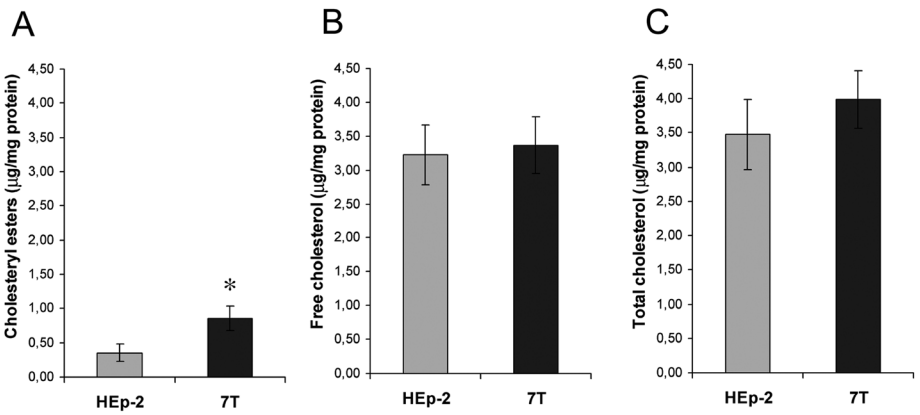

Fig. 4 Determination of cholesteryl esters (A), free cholesterol (B) and (C) total cholesterol in HEp-2 and 7T cells. The cells were grown in a 6 well plate for 48 h and thereafter the Amplex Red Cholesterol Assay Kit was used following manufacturer's protocol. Cholesteryl esters were determined by the difference between total and free cholesterol. Means and ± SEM of 4 independent experiments, each performed in triplicate, are shown. *$p < 0.05$.

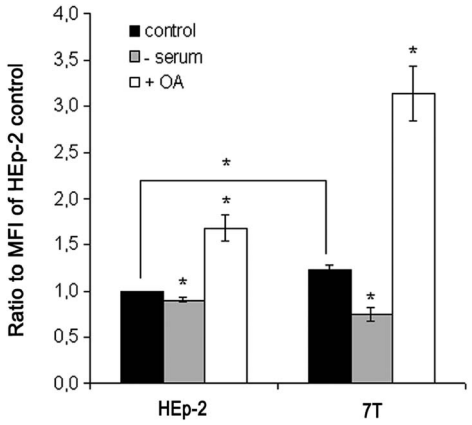

Fig. 6 Determination of lipid droplets in HEp-2 and 7T cells by Nile Red staining. 24 h after seeding, cells were incubated for an additional 24 h in medium with serum (control), medium without serum (−serum) or medium with serum and 200 μM oleic acid (+OA). Following the treatment, cells were stained with Nile Red and the mean fluorescence intensity (MFI) was immediately analyzed with a FACSCalibur flow cytometer. The results were obtained from four independent measurements. All values are expressed relative to MFI values of HEp-2 control cells (67.03 ± 8.36), set at 1.0. *$p < 0.05$.

which bind to LDs due to their nonpolar nature.[34] The results of Oil Red O staining (Fig. 5) showed that LDs could be visualized as red colored dots only in the resistant 7T cells, and they disappeared upon serum withdrawal. At the same time, no visible dots could be detected in parental HEp-2 cells if they were grown in media with or without the serum. Since LDs can vary in size and can be very small and hardly detectable,[35,36] we used a more sensitive and quantitative method for LD detection, *i.e.* flow cytometric detection with Nile Red staining.[37] The results of Nile Red staining are presented in Fig. 6. Higher Nile Red fluorescence was detected in 7T cells as compared to HEp-2 cells. When serum was deprived from growth media, a larger decrease in Nile Red fluorescence was detected in 7T cells. Supplementation of serum with oleic acid at a nontoxic concentration (as verified by MTT assay, data not shown) induced more Nile Red fluorescence in 7T cells as compared to HEp-2 cells. Therefore, flow cytometric data show that LDs are indeed present inside the 7T cells, while HEp-2 cells have a very small amount of LDs. In addition, supplementation of serum with oleic acid implies that 7T cells have higher potential to increase the amount of lipid droplets compared to HEp-2 cells, suggesting possible alterations in the mechanism of lipid droplet formation in 7T cells.

Discussion

The infrared (IR) spectrum of a cell comprises vibrational spectra of all molecules present in the cell and is one of the most information-rich and concise ways to represent the nature and quantities of all molecules present in the cell and, as such, has provided the development of FTIR spectroscopy as a useful and promising method in cancer research.[2] The identification and assignment of IR spectral components (marker peaks) are generally performed by the so-called "group frequency approach" which is a traditional and quite popular method of spectral analysis. The frequency of vibration of specific functional groups is pre-assigned according to those observed in the IR spectrum of the corresponding pure biomolecules[38] or mixtures of molecules[39] and compared with those already reported in the literature.[40] Nevertheless, the IR spectrum of a cell usually contains a large number of bands, many of which are impossible to be confidently assigned to vibration of a particular group since vibrations of different molecular components of a cell overlap (see Table 1, "Spectral assignment" column) and the spectrum reflects only the average biochemical composition.[2] Therefore, we must conclude that the unequivocal interpretation of pre-assigned vibrational frequencies of cell spectra is difficult and it requires the application of some type of "resolution enhancement". One way to do this is the calculation of difference spectrum which gives information on biochemical, functional, structural and dynamical changes occurring in complex samples and in some circumstances enables identification of spectral components that may give useful information about the system explored. For example, during the treatment of the human prostate cancer PC-3 cell line with cardiotonic steroids[23] FTIR difference spectra revealed a relative increase in the amount of lipids with respect to the other cell components. Since cardiotonic steroids represent a group of compounds that bind to the membrane embedded sodium pump,[41] this finding was new and interesting. After lipid isolation and analysis, a modification in the nature of cell lipids was found, which suggested an additional mechanism of action for cardiotonic steroids in cancer cells.

Based on this approach, we decided to use FTIR spectral analysis to generally examine all molecular changes present in resistant 7T cells with intention to find some new candidates involved in drug resistance. To do this, we first examined whether FTIR spectra of 7T cells, which reflect global macromolecular changes that occurred in this drug resistant cell line, could be distinguishable from the FTIR spectra of the sensitive HEp-2 cell line. PCA and hierarchical clustering (Fig. 1 and 2) showed a clear difference between FTIR spectra of these two lines. Our results are in accordance with other results obtained previously with different types of resistant and sensitive cancer cell line pairs.[4,5,8–10] Second, we wanted to identify the biochemical changes in resistant 7T cells as compared to parental HEp-2 cells by making difference spectra and spectral assignment of the peaks where differences were most pronounced. In this way we found that two major classes of molecules (lipids and proteins) are less abundant in 7T cells. We can also support this conclusion by the additional analysis of overall difference spectra shape regardless of the statistically relevant areas. Namely, if we look at the difference spectra shape in the area under the curve between 3000 and 2800 cm^{-1} (Fig. 3), which is dominated by the contribution of hydrocarbon chains of the lipids,[2] all the peaks are negative suggesting a decrease in the amount of lipids in 7T resistant cells. In addition, both amide I and amide II peaks in the area under the curve between 1650 and 1540 cm^{-1} (Fig. 3), which is attributable to both α-helical and β-sheet secondary protein structures,[42] are

also negative suggesting a decrease in the general amount of proteins in 7T resistant cells (Fig. 3). Furthermore, the area, which is a part of the "fingerprinting region"[2] and spans over 1400 to 1340 cm^{-1} where lipid and protein absorptions overlap, is also negative suggesting again a decrease in both lipids and proteins in 7T cells (Fig. 3). All presented findings support our previous conclusion based on statistical analysis that lipids and proteins are less abundant in resistant 7T cells.

One possible explanation for the lower lipid content that was found in 7T resistant cells is the smaller size of 7T cells as compared to HEp-2 cells, which was determined in our previous study by measuring the cell size on a Beckman Cell Counter and on flow cytometric histograms of cell size distribution.[20] We presume that, if cells are smaller in size *i.e.* have smaller volume, they will also have a smaller surface of the cell membrane and thus less lipids in general. We could support this presumption with the fact that after staining HEp-2 and 7T cells with DiI, a carbocyanine dye which fluoresces upon binding to the cellular phospholipid bilayer,[43] 7T cells had a lower fluorescence intensity compared to HEp-2 cells, as detected by flow cytometry (data not shown). The smaller cell size could also explain the lower protein content found in 7T cells. Additionally, the lower protein content of 7T cells could be explained by a slower growth rate of 7T cells compared to HEp-2 cells.[20] Namely, in a recent article a correlation analysis was performed which spanned over 60 different cell lines and it was found that higher expression of the protein translational machinery, including the preprocessing of mRNAs, has a very straightforward quantitative relationship with higher proliferation rates of different cancer cells.[44]

In short, the data obtained by analysis of difference spectra are implying that 7T cells, probably due to a smaller cell size and lower proliferation rate compared to HEp-2 cells, have a lower amount of lipids and proteins in general, confirming the data that we obtained previously with more specific methods.[20] Alongside these results, the FTIR technique identified some additional alterations in 7T cells. It detected the increase in two areas of difference spectra located around ~1735 cm^{-1} and 1170–1130 cm^{-1} with mutual spectral annotation to cholesteryl esters (Table 1) thus suggesting the changes in their amount. These data were verified with enzymatic assay which detected a two fold increase in the cholesteryl esters mass in 7T resistant cells as compared to HEp-2 parental cells (Fig. 4A). It is interesting to note that the quantity of cholesteryl esters in both cell lines was quite low compared to the level of cholesterol (Fig. 4B and C). In addition, these data suggest that FTIR spectroscopy is quite a sensitive method that can detect very small amounts of molecules.

Cholesteryl esters are molecules localized in special cytoplasmic organelles called lipid droplets.[32] In the recent literature there have been several review articles which summarized the role of cholesteryl esters and lipid droplets in the processes of cancer development and progression.[45–47] In addition, the increase in cholesteryl ester formation and the presence of lipid droplets were reported in several drug resistant cell lines. For example, the human ovarian carcinoma cell line resistant to cisplatin (C13) showed higher lipid accumulation mainly within cytoplasmic droplets in comparison to the cisplatin-sensitive (2008) cell line.[48] In doxorubicin resistant human mammary carcinoma MCF-7 cells and human colon adenocarcinoma LoVo cells the increased amount of esterified cholesterol, saturated cholesteryl ester and triglyceride fatty acid was found as compared to their sensitive counterparts.[49,50] Similarly, when the doxorubicin resistant MCF-7R subline and the doxorubicin resistant human oral epidermoid carcinoma KBR subline, as well as the human promyelocytic leukemia vincristine resistant HL60R subline were compared with their sensitive cell counterparts, an increase in cytoplasmic organelles that stain with Nile Red was observed,[51] which is a main characteristic of lipid droplet staining. In our study, the detection of lipid droplets by Oil Red O and Nile Red staining showed that drug resistant 7T cells have a higher amount of lipid droplets present in the cytoplasm and also have a higher capacity to increase their amount due to free fatty acid stimulation, compared to the parental laryngeal carcinoma HEp-2 cell line.

The exact role of cholesteryl esters and lipid droplets in drug resistance has not yet been resolved. Some possible mechanisms are emerging from a recent study where it was shown that progestins in progesterone receptor positive breast cancer T47D cells induced lipid droplet formation and reduced sensitivity to docetaxel.[52] Even more, it was found that intact docetaxel molecules were present within progestin induced lipid droplets, suggesting a protective quenching effect of intracellular lipid droplets. Regarding our recent research of curcumin resistance in 7T cells,[20] it would be interesting to explore if curcumin, which is a hydrophobic compound like docetaxel,[53] would accumulate inside of lipid droplets present in 7T resistant cells and if modulation of lipid droplet quantity could affect resistance to that compound.

Conclusions

The FTIR technique has become a very useful and promising tool in cancer research and diagnostics, and has also shown to be quite useful in the present study of basic research when exploring the molecular mechanisms involved in drug resistance. The FTIR technique combined with Kinetics software provided an overall signature of all molecules whose quantity changed in drug resistant carcinoma 7T cells compared to parental HEp-2 cells, but also information about alteration in the quantity of some specific molecules, like cholesteryl esters. However, it needs to be taken into account that, during interpretation of results based on spectral assignments, at least two or more peaks with the same orientation and the same spectral assignment should be used to identify the molecules and then verified with more specific methods.

Our finding about the increase in the cholesteryl ester quantity and the amount of lipid droplets in drug resistant cells suggests that these molecules and cell structures might have some role in tumor cell drug resistance which has not yet been resolved, and should merit more exploration in the future as potential biomarkers of drug resistance or therapeutic targets for drug resistant tumors. Finally, our data imply that FTIR spectroscopy is quite a sensitive method that is not only able to

detect which types of molecules are changed in quantity when comparing two sets of samples, but also quite sensitive in detecting very small amounts of these molecules.

Abbreviations

ATR	Attenuated total reflection
FTIR	Fourier transform infrared
IR	Infrared
LD	Lipid droplets
MFI	Mean fluorescence intensity
OA	Oleic acid
PC	Principal component
PCA	Principal component analysis
ROS	Reactive oxygen species

Acknowledgements

This work was supported by the funds from the Ministry of Science, Education and Sport of the Republic of Croatia (Project 098-0982913-2748). We want to give special thanks to Prof. Erik Goormaghtigh who provided us with the specific "homemade" program Kinetics and very useful knowledge about the FTIR technique. We thank Mrs A. Tupek and Mrs S. Juler for the technical assistance.

References

1 H. Zahreddine and K. L. Borden, *Front Pharmacol.*, 2013, **4**, 28.
2 G. Bellisola and C. Sorio, *Am. J. Cancer Res.*, 2012, **2**, 1–21.
3 J. M. Le Gal, H. Morjani, O. Fardel, A. Guillouzo and M. Manfait, *Anticancer Res.*, 1994, **14**, 1541–1548.
4 J. M. Le Gal, H. Morjani and M. Manfait, *Cancer Res.*, 1993, **53**, 3681–3686.
5 G. Bellisola, G. Cinque, M. Vezzalini, E. Moratti, G. Silvestri, S. Redaelli, C. Gambacorti Passerini, K. Wehbe and C. Sorio, *Analyst*, 2013, **138**, 3934–3945.
6 A. Zwielly, S. Mordechai, G. Brkic, E. Bogomolny, I. Z. Pelly, R. Moreh and J. Gopas, *Eur. Biophys. J.*, 2011, **40**, 795–804.
7 A. Zwielly, J. Gopas, G. Brkic and S. Mordechai, *Analyst*, 2009, **134**, 294–300.
8 C. M. Krishna, G. Kegelaer, I. Adt, S. Rubin, V. B. Kartha, M. Manfait and G. D. Sockalingum, *Biopolymers*, 2006, **82**, 462–470.
9 C. Murali Krishna, G. Kegelaer, I. Adt, S. Rubin, V. B. Kartha, M. Manfait and G. D. Sockalingum, *Biochim. Biophys. Acta*, 2005, **1726**, 160–167.
10 A. Gaigneaux, J. M. Ruysschaert and E. Goormaghtigh, *Eur. J. Biochem.*, 2002, **269**, 1968–1973.
11 C. Petibois, B. Drogat, A. Bikfalvi, G. Deleris and M. Moenner, *FEBS Lett.*, 2007, **581**, 5469–5474.
12 J. R. Mourant, K. W. Short, S. Carpenter, N. Kunapareddy, L. Coburn, T. M. Powers and J. P. Freyer, *J. Biomed. Opt.*, 2005, **10**, 031106.
13 J. R. Mourant, J. Dominguez, S. Carpenter, K. W. Short, T. M. Powers, R. Michalczyk, N. Kunapareddy, A. Guerra and J. P. Freyer, *J. Biomed. Opt.*, 2006, **11**, 064024.
14 C. Ceylan, A. Camgoz and Y. Baran, *Technol. Cancer Res. Treat.*, 2012, **11**, 333–344.
15 Y. Baran, C. Ceylan and A. Camgoz, *Biomed. Pharmacother.*, 2013, **67**, 221–227.
16 J. J. Lu, Y. J. Cai and J. Ding, *Mol. Cell. Biochem.*, 2012, **360**, 253–260.
17 B. Sung, A. B. Kunnumakkara, G. Sethi, P. Anand, S. Guha and B. B. Aggarwal, *Mol. Cancer Ther.*, 2009, **8**, 959–970.
18 M. Labbozzetta, M. Notarbartolo, P. Poma, A. Maurici, L. Inguglia, P. Marchetti, M. Rizzi, R. Baruchello, D. Simoni and N. D'Alessandro, *Ann. N. Y. Acad. Sci.*, 2009, **1155**, 278–283.
19 N. M. Weir, K. Selvendiran, V. K. Kutala, L. Tong, S. Vishwanath, M. Rajaram, S. Tridandapani, S. Anant and P. Kuppusamy, *Cancer Biol. Ther.*, 2007, **6**, 178–184.
20 S. Rak, T. Cimbora-Zovko, G. Gajski, K. Dubravcic, A. M. Domijan, I. Delas, V. Garaj-Vrhovac, D. Batinic, J. Soric and M. Osmak, *Toxicol. In Vitro*, 2013, **27**, 523–532.
21 M. Osmak, L. Bizjak, B. Jernej and S. Kapitanovic, *Mutat. Res.*, 1995, **347**, 141–150.
22 E. Goormaghtigh, V. Raussens and J. M. Ruysschaert, *Biochim. Biophys. Acta*, 1999, **1422**, 105–185.
23 R. Gasper, J. Dewelle, R. Kiss, T. Mijatovic and E. Goormaghtigh, *Biochim. Biophys. Acta*, 2009, **1788**, 1263–1270.
24 A. Gaigneaux, J. M. Ruysschaert and E. Goormaghtigh, *Appl. Spectrosc.*, 2006, **60**, 1022–1028.
25 P. Greenspan, E. P. Mayer and S. D. Fowler, *J. Cell Biol.*, 1985, **100**, 965–973.
26 G. Cakmak, I. Togan and F. Severcan, *Aquat. Toxicol.*, 2006, **77**, 53–63.
27 C. S. Colley, S. G. Kazarian, P. D. Weinberg and M. J. Lever, *Biopolymers*, 2004, **74**, 328–335.
28 J. Hayashi, T. Saito and K. Aizawa, *Lasers Surg. Med.*, 1997, **21**, 287–293.
29 F. Le Naour, M. P. Bralet, D. Debois, C. Sandt, C. Guettier, P. Dumas, A. Brunelle and O. Laprevote, *PLoS One*, 2009, **4**, e7408.
30 N. S. Ozek, S. Tuna, A. E. Erson-Bensan and F. Severcan, *Analyst*, 2010, **135**, 3094–3102.
31 C. Stoll, J. L. Holovati, J. P. Acker and W. F. Wolkers, *Mol. Membr. Biol.*, 2011, **28**, 454–461.
32 T. Fujimoto and R. G. Parton, *Cold Spring Harbor Perspect. Biol.*, 2011, **3**, a004838.
33 A. A. Spector, S. N. Mathur, T. L. Kaduce and B. T. Hyman, *Prog. Lipid Res.*, 1980, **19**, 155–186.
34 R. C. Melo, H. D'Avila, P. T. Bozza and P. F. Weller, *Methods Mol. Biol.*, 2011, **689**, 149–161.
35 Y. Ohsaki, J. Cheng, M. Suzuki, Y. Shinohara, A. Fujita and T. Fujimoto, *Biochim. Biophys. Acta*, 2009, **1791**, 399–407.
36 A. R. Thiam, R. V. Farese, Jr and T. C. Walther, *Nat. Rev. Mol. Cell Biol.*, 2013, **14**, 775–786.
37 A. Gubern, J. Casas, M. Barcelo-Torns, D. Barneda, X. de la Rosa, R. Masgrau, F. Picatoste, J. Balsinde, M. A. Balboa and E. Claro, *J. Biol. Chem.*, 2008, **283**, 27369–27382.

38 A. Pevsner and M. Diem, *Biopolymers*, 2003, **72**, 282–289.
39 E. Benedetti, E. Bramanti, F. Papineschi, I. Rossi and E. Benedetti, *Appl. Spectrosc.*, 1997, **51**, 792–797.
40 Z. Movasaghi, S. Rehman and U. Rehman, *Appl. Spectrosc. Rev.*, 2008, **43**, 134–179.
41 T. Mijatovic, E. Van Quaquebeke, B. Delest, O. Debeir, F. Darro and R. Kiss, *Biochim. Biophys. Acta*, 2007, **1776**, 32–57.
42 E. Goormaghtigh, J. M. Ruysschaert and V. Raussens, *Biophys. J.*, 2006, **90**, 2946–2957.
43 F. Progatzky, M. J. Dallman and C. Lo Celso, *Interface Focus*, 2013, **3**, 20130001.
44 A. Feizi and S. Bordel, *Sci. Rep.*, 2013, **3**, 3041.
45 P. T. Bozza and J. P. Viola, *Prostaglandins, Leukotrienes Essent. Fatty Acids*, 2010, **82**, 243–250.
46 E. J. Delikatny, S. Chawla, D. J. Leung and H. Poptani, *NMR Biomed.*, 2011, **24**, 592–611.
47 M. R. Tosi and V. Tugnoli, *Clin. Chim. Acta*, 2005, **359**, 27–45.
48 M. Montopoli, M. Bellanda, F. Lonardoni, E. Ragazzi, P. Dorigo, G. Froldi, S. Mammi and L. Caparrotta, *Curr. Cancer Drug Targets*, 2011, **11**, 226–235.
49 M. T. Santini, M. Napolitano, A. Ferrante, G. Rainaldi, G. Arancia and E. Bravo, *Anticancer Res.*, 2003, **23**, 4737–4746.
50 M. T. Santini, R. Romano, G. Rainaldi, P. Filippini, E. Bravo, L. Porcu, A. Motta, A. Calcabrini, S. Meschini, P. L. Indovina and G. Arancia, *Biochim. Biophys. Acta*, 2001, **1531**, 111–131.
51 H. Morjani, N. Aouali, R. Belhoussine, R. J. Veldman, T. Levade and M. Manfait, *Int. J. Cancer*, 2001, **94**, 157–165.
52 I. R. Schlaepfer, C. A. Hitz, M. A. Gijon, B. C. Bergman, R. H. Eckel and B. M. Jacobsen, *Mol. Cell. Endocrinol.*, 2012, **363**, 111–121.
53 Y. Liu, Y. Mi, J. Zhao and S. S. Feng, *Int. J. Pharm.*, 2011, **421**, 370–378.